Reliability Engineering and System Safety 270 (2026) 112187

Contents lists available at ScienceDirect

Reliability Engineering and System Safety

journal homepage: www.elsevier.com/locate/ress

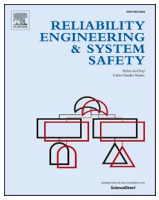

Reliability-Based Maintenance Optimization of Reusable Phased Mission Systems

Xiang-Yu Li [a], Haochen Wang [a], He Li [b,*], Xiaoyan Xiong [a], Zaili Yang [b], Hong-Zhong Huang [c], Michael Beer [d,e,f], Jin Wang [b]

[a] Key Laboratory of Advanced Transducers and Intelligent Control System, Ministry of Education, Taiyuan University of Technology, 030024 Taiyuan, China
[b] Liverpool Logistics, Offshore and Marine (LOOM) Research Institute, Liverpool John Moores University, Liverpool, UK
[c] Center for System Reliability and Safety, University of Electronic Science and Technology of China, 611731 Chengdu, China
[d] Institute for Risk and Reliability, Leibniz Universität Hannover, Hannover 30167, Germany
[e] Department of Civil and Environmental Engineering, University of Liverpool, Liverpool L69 3GH, UK
[f] International Joint Research Center for Resilient Infrastructure & International Joint Research Center for Engineering Reliability and Stochastic Mechanics, Tongji University, Shanghai 200092, China

ARTICLE INFO

Keywords:
Maintenance
Reliability modeling
Reusable phased mission systems
Multi-phased Wiener process

ABSTRACT

This paper proposes a reliability-based maintenance optimization method for reliability modeling and maintenance planning of reusable phased mission systems (R-PMSs). Initially, a multi-phased Wiener process-based reliability modeling method, combined with the Binary Decision Diagram-based model, is created to assess the reliability of R-PMSs. The method considers the initial states of components to be perfect/imperfect fixed as a basis to reflect the impacts of multiple usages of R-PMSs. Subsequently, a maintenance optimization model based on the reliability assessed and incorporating multiple maintenance actions is constructed to allocate the maintenance resources into the maintenance activities in advance of subsequent missions of R-PMSs. The model balances the maintenance cost, overall reliability, and task requirements. The superiority and performance of the proposed method are validated by numerical and engineering analysis. The results confirmed that the proposed method contributes to reliability modeling and maintenance scheduling of R-PMSs.

1. Introduction

Recent decades have seen a surge in the development of reliability modeling and maintenance optimization of Phased Mission Systems (PMSs), which segments the overall operational lifetime into distinct time intervals, referred to as phases [1]. Advances in reliability modeling [2], reliability analysis [3], reliability assessment [4] and redundancy optimization [5] supported the PMSs stepping into real applications such as aerospace [6], nuclear power [7], computing systems [8], robotics [9], electric industry [10], and medical equipment [11].

The newly emerged reusable systems, however, challenging the well-established knowledge systems in terms of PMSs, which transform the PMSs from a single-use to a multiple-use nature, are referred to as Reusable Phased Mission Systems (R-PMSs). Typical examples include the reusable Launch Vehicles [12], and the Reusable autonomous Underwater Vehicle [13]. In traditional PMSs, system reliability is required to ensure reliability for a single use. Differently, apart from the system reliability, maintenance scheduling becomes another core consideration of the R-PMSs' lifelong management. Accordingly, the reliability-centered maintenance of R-PMSs is built upon maintaining the required system reliability of each phase of a specific mission as well as the entire task, which includes several series of missions. It is pointed out that the maintenance scheduling with limited resources (maintenance time and cost) and reliability modeling are the key to reliability-centered maintenance of R-PMSs [14,15],[16].

Maintenance actions ensure the recovery of failed or degraded components and sustain the system in a safer operational condition [17]. A well-designed maintenance strategy improves system reliability while reducing the lifetime maintenance expenses [18],[19]. To be specified, the efforts on maintenance planning of PMSs include: (i) Multistate Systems [20]. The core for maintenance planning of such systems is to handle the system performance degradation, dynamic task requirements, and resource constraints. For instance, the joint

* Corresponding Author.
E-mail address: h.li@ljmu.ac.uk (H. Li).

https://doi.org/10.1016/j.ress.2026.112187
Received 19 June 2025; Received in revised form 28 December 2025; Accepted 1 January 2026
Available online 6 January 2026

optimization of redundancy and maintenance [21] and predictive maintenance based on dynamic tasks [22]; (ii) S-dependent Systems [23,24]. It emphasizes the interrelationships among subsystems or tasks, and the maintenance strategies of which map task offloading, resource allocation, and collaborative optimizations. For example, the reflection of s-dependent competitive risks among components through Copula [25] and the construction of reliability-centered multi-level maintenance optimization models [26]; and (iii) Various System Durations [27]. The key efforts are to understand the impact of variable task execution time on the ultimate optimized maintenance strategies. For instance, selective maintenance concepts to handle the situation where both rest time and task time are random variables [28], there are uncertainties [29] from environmental fluctuations, random component degradation, etc., according to probability models and intelligent predictions. Special cases include predictive maintenance based on multi-source information fusion and deep reinforcement learning [30] as well as reinforcement learning, genetic algorithm simulation, heuristic methods, and scheduling rules [31]. It is highlighted that the reliability-centered maintenance relies on the scientific and convincing reliability modeling and assessment, which acts as the foundation of maintenance planning.

Reliability modeling and assessment of PMSs lie in addressing the phase dependency. For instance, in non-repairable PMSs, a component that fails during an earlier phase remains in a failed state in subsequent phases. Simulation methods [32], combinatorial methods [33], state-space models and modular methods [34] are adequate in handling phase dependencies of PMSs. To be specific, a very early approximation methodology [9] is put forward for reliability modeling of PMSs. After that, -the fault tree-based method [3] and Markov process-based method [4] are jointly proposed for a detailed and convincing reliability modeling of PMSs. Recent years have seen the development of Binary Decision Diagram-based (BDD-based) methods that are able to significantly enhance the efficiency of reliability modeling. For instance, a Markov regenerative process (MRGP) based method [35] is developed to deal with the non-exponential multi-state non-exponential components in different working phases. A redundancy allocation strategy for PMSs with the mixed redundancy strategy and backup missions [36] is generated to consider internal and external shocks. Additionally, new sampling methods [37] and PMS that leverage the BDD (PMS-BDD) method [38] are applicable when the scale of systems and phases becomes large. It is highlighted that epistemic uncertainties quantification models [39] and reliability models considering common cause failures [40] are also promising concepts in addressing system complexities.

In most of the existing research, reliability modeling techniques assign components/systems a perfect working state at the beginning of each mission and a specified life distribution to each component. The mentioned modeling mechanisms are capable of modeling the reliability of single-use PMSs, but fail to address their multiple usage and the interactions of maintenance actions. Meanwhile, most of the existing maintenance optimization concepts have been well constructed based on a single-round mission, which shows insufficiency in handling the optimization problems of R-PMS. To this end, this paper proposes a reliability-based maintenance optimization method for R-PMSs, extending the PMS-targeted reliability-centered maintenance to R-PMSs. The novel contributions of this paper are as follows,

- A multi-phased stochastic process-based model accurately captures component degradation propagation across successive missions, overcoming the limitations of mission-independent modeling. The method demonstrates strong parameter robustness and practical applicability.
- An efficient probabilistic evolution method resolves the state-space explosion problem by tracking key state expectations, transforming path enumeration into tractable probability evaluation. This approach maintains high accuracy while improving computational efficiency by an order of magnitude.
- Maintenance optimization is achieved through intelligent determination of component-specific thresholds for preventive maintenance and replacement. This adaptive strategy enables condition-based decision-making, significantly enhancing resource utilization while ensuring reliability requirements.

Overall, this paper proposes a novel framework for reliability-centered maintenance to deal with the practical needs of newly emerged R-PMSs, which, from the academic point of view, updates the existing knowledge in terms of PMSs till it can deal with the reusable nature of R-PMSs. The reminder is organized as follows. Section 2 introduces methodology. Section 3 demonstrates the effectiveness and applicability of the proposed methods. Conclusions and future works are provided in Section 4.

2. Methodology

This section proposes a reliability-centered maintenance optimization framework to provide a systematic basis for maintenance scheduling and resource allocation for the R-PMSs. The methodology is structured into three sections: (i) problem formulation and key assumptions, (ii) reliability modeling of components/systems combining multi-phased Wiener process and BDD model, and (iii) maintenance modeling and optimization under both unlimited and limited mission scenarios.

2.1. Problem Descriptions and Assumptions

The R-PMSs are systems designed to accomplish multiple missions and each mission can be divided into several phases. The success of each mission is the production of all successful phases. The assumptions are as follows:

#1. Assumptions in terms of system reliability

- The R-PMS executes a series of phases. The operation parameters and failure criteria of components are different in various phases.
- Components are new at the beginning of the first phase of the first mission, with the reliability equal to one, which degrades (less than one) in the subsequent kth$(k \geq 2)$ phases.

#2. Assumptions regarding maintenance

- The maintenance actions can be, and only be, carried out between two concecutive missions.
- Preventive Maintenance (PM) threshold $L_{1,i}$ and the Replace (RE) threshold $L_{2,i}$ $(L_{1,i} < L_{2,i})$ collaboratively guide maintenance activities. Replacement of a component takes place in case the degradation meets $x \geq L_{2,i}$; repair of a component takes place if the component's degradation follows $L_{1,i} \leq x < L_{2,i}$; there are no maintenance actions towards components if the degradation meets$x < L_{1,i}$.

2.2. Reliability modeling of R-PMS

2.2.1. Multi-phased Wiener process for reliability modeling of a component

The Wiener process reflects the degradation process of components or systems in both monotonic and non-monotonic behaviors. In this section, a multi-phased Wiener process-based approach is proposed for component reliability modeling, accounting for varying degradation characteristics across phases. To be specific, the Wiener process reflects the degradation by $X(t)$, which is computed by:

$$X(t) = x_0 + \mu t + \sigma B(t) \tag{1}$$

where, x_0, μ, and σ are initial degradation, drift, and diffusion coefficient, $B(t)$ is a standard Brownian motion. Accordingly, the failure time

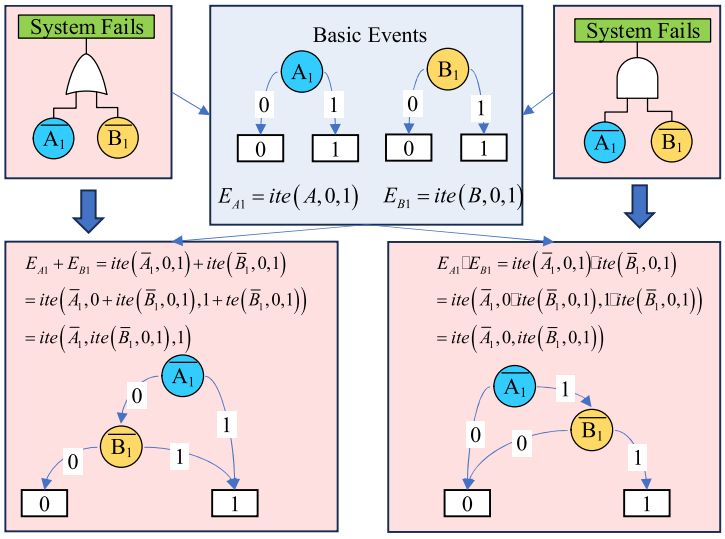

Figure 1. The phase BDD model construction process with series and parallel systems/$index(A_1) < index(B_1)$ and A_i are variables related to component A in the phase.

is defined by the First Passage Time (FPT). And the PDF functions of the FPT could be presented by the Inverse Gaussian distribution. For instance, Qian et al. [41] combined the nonlinear Wiener process with a Copula function for effective predictions. Accordingly, the FPT in this paper can be computed by:

$$f(t|x,\mu,\sigma,D_{\max}) = \frac{D_{\max}-x}{\sqrt{2\pi\sigma^2 t^3}}\exp\left(-\frac{(D_{\max}-x-\mu t)^2}{2\sigma^2 t}\right) \tag{2}$$

$D_{\max}$ and x represent the failure threshold and initial degradation, respectively. Components operate across multiple phases, each characterized by a distinct working environment that results in various operational stresses and degradation behaviors. The degradation of components is continuous throughout several phases. Hence, the multi-phased Wiener process is used to model the multi-phased degraded nature of components. Extend from Eq. (1), the degradation $X(t)$ of a multi-phased Wiener process is expressed by:

$$X(t) = \begin{cases} \widehat{X}_1 + \mu_1 t + \sigma_1 B(t) & 0 < t \le T_1 \\ \widehat{X}_2 + \mu_2 t + \sigma_2 B(t) & T_1 < t \le T_1 + T_2 \\ \widehat{X}_3 + \mu_3 t + \sigma_3 B(t) & T_1 + T_2 < t \le T_1 + T_2 + T_3 \\ \cdots \end{cases} \tag{3}$$

where, μ_i and σ_i denote the drift and diffusion coefficients of the component in phase i, T_i is the duration time of phase i. μ_i and σ_i remain the same due to the stable operational and environmental conditions within the phases. $\widehat{X}_i$ represents the initial degradation of the component for phase i. It is obvious that $\widehat{X}_i = X\left(\sum_{j=1}^{i-1} T_j\right), (i > 2)$. Combined Eqs. (2) and (3), the PDF function for FPT in the multi-phased Wiener process could be derived as:

$$f(t) = \begin{cases} f_1(t|\widehat{X}_1,\mu_1,\sigma_1,0,D_{\max}), & 0 < t \le T_1 \\ f_1(t|\widehat{X}_2,\mu_2,\sigma_2,T_1,D_{\max}), & T_1 < t \le T_1 + T_2 \\ f_1(t|\widehat{X}_3,\mu_3,\sigma_3,T_1+T_2,D_{\max}), & T_1 + T_2 < t \le T_1 + T_2 + T_3 \\ \cdots \end{cases}$$

$$f_1(t|x,\mu,\sigma,\tau,D_{\max}) = \frac{D_{\max}-x}{\sqrt{2\pi\sigma^2(t-\tau)^3}}\exp\left(-\frac{(D_{\max}-x-\mu(t-\tau))^2}{2\sigma^2(t-\tau)}\right) \tag{4}$$

With the PDF shown in Eq. (4), the component's CDF and reliability functions could be derived, shown as:

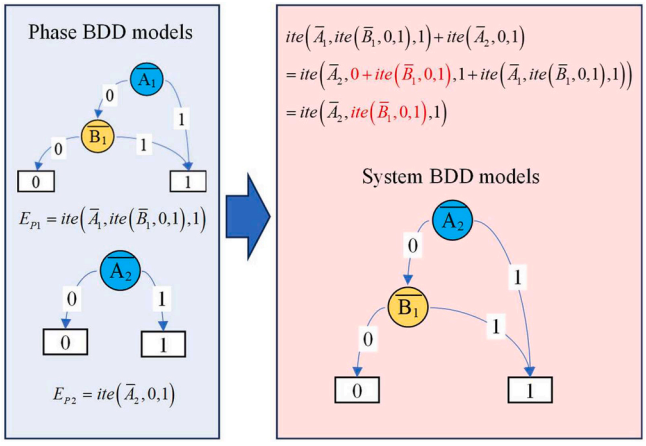

Figure 2. The phase BDD system model construction process.

$$F(t) = \int_0^t f_1(s)ds, \qquad R(t) = 1 - F(t)$$

$$f_2(t|x,\sigma,\mu,\tau,D_{\max}) = 1 - F(t)$$

$$= 1 - \int_0^t \frac{D_{\max}-x}{\sqrt{2\pi\sigma^2(s-\tau)^3}}\exp\left(-\frac{(D_{\max}-x-\mu(s-\tau))^2}{2\sigma^2(s-\tau)}\right)ds$$

$$= \Phi\left(\frac{D_{\max}-x-\mu(t-\tau)}{\sigma\sqrt{t-\tau}}\right) - \exp\left(\frac{2\mu(D_{\max}-x)}{\sigma^2}\right)\Phi\left(\frac{x_0-D_{\max}-\mu(t-\tau)}{\sigma\sqrt{t-\tau}}\right) \tag{5}$$

Then, the reliability function for the multi-phased Wiener process is,

$$R(t) = \begin{cases} f_2(t|\widehat{X}_1,\mu_1,\sigma_1,0,D_{\max}), & 0 < t \le T_1 \\ f_2(t|\widehat{X}_2,\mu_2,\sigma_2,T_1,D_{\max}), & T_1 < t \le T_1 + T_2 \\ f_2(t|\widehat{X}_3,\mu_2,\sigma_2,T_1+T_2,D_{\max}), & T_1 + T_2 < t \le T_1 + T_2 + T_3 \\ \cdots \end{cases} \tag{6}$$

Eq. (6) indicates that, in phase one, the initial degradation x_0 and parameters μ_1, σ_1, and $D_{\max}$ are known values. However, for phases $i(i > 2)$, the initial degradation is equal to that at the end of the last phase, $\widehat{X}_i = X\left(\sum_{j=1}^{i-1} T_j\right)$, which is an unknown value. The degradation

increment in phases $i(i>2)$ follows a normal distribution, with expectation $\widehat{X}_i+\mu_i T_i$ and variance $\sigma_i^2 T_i$. With Brownian bridge, the probability that the degradation increases from $\widehat{X}_i$ to x under $D_{\max}$ could be expressed as,

$$f_3(\widehat{X}_i|t,\widehat{X}_{i-1},\mu_i,\sigma_i,D_{\max}) = \begin{cases} \frac{1}{\sigma_i\sqrt{t}}\phi\left(\frac{x-\widehat{X}-\mu_i t}{\sigma_i\sqrt{t}}\right)\left[1-\exp\left(-\frac{2(D_{\max}-\widehat{X}_i)(D_{\max}-\widehat{X}_{i-1})}{\sigma_i^2 t}\right)\right], & \max(\widehat{X}_i,\widehat{X}_{i-1})<D_{\max} \\ 0, & \max(\widehat{X}_i,\widehat{X}_{i-1})\geq D_{\max} \end{cases} \tag{7}$$

It should be noted that the first part in Eq.(7) is the normal distribution for the degradation, and the second part ensures that the degradation x does not exceed $D_{\max}$. So the pdf function for the degradation at the end of each phase could be derived as,

$$f(\widehat{X}_i) = \begin{cases} f_3(\widehat{X}_1|t-T_1,x_0,\mu_2,\sigma_2,D_{\max}), & 0<t\leq T_1 \\ \int_0^D f_3(\widehat{X}_2|t-T_1,\widehat{X}_1,\mu_2,\sigma_2,D_{\max})f(\widehat{X}_1)d\widehat{X}_1, & T_1<t\leq T_1+T_2 \\ \int_0^D f_3(\widehat{X}_3|t-(T_1+T_2),\widehat{X}_2,\mu_3,\sigma_3,D_{\max})f(\widehat{X}_2)d\widehat{X}_2, & T_1+T_2<t\leq T_1+T_2+T_3 \\ \cdots \end{cases} \tag{8}$$

Integrating Eqs. (6) and (8), the component reliability could be derived as:

$$R(t) = \begin{cases} f_2(t|\widehat{X}_1,\mu_1,\sigma_1,0,D_{\max}), & 0<t\leq T_1 \\ \int_0^D f_2(t|\widehat{X}_2,\mu_2,\sigma_2,0,D_{\max})f(\widehat{X}_2)d\widehat{X}_2, & T_1<t\leq T_1+T_2 \\ \int_0^D f_2(t|\widehat{X}_3,\mu_3,\sigma_3,0,D_{\max})f(\widehat{X}_3)d\widehat{X}_3, & T_1+T_2<t\leq T_1+T_2+T_3 \\ \cdots \end{cases} \tag{9}$$

2.2.2. Reliability modeling of R-PMS

The system reliability of PMSs is modeled by PMS-BDD with the assistance of the components' reliability computed in Section 2.2.1. The PMS-BDD model includes the following steps:

Step #1. Construct phase BDD models (a directed acyclic graph decomposes Boolean functions, see [1]) based on the Reliability Block Diagram (RBD) models. The construction process for series and parallel systems is displayed in Figure 1. Terminal nodes (the success/failure of the whole system is denoted by 0/1), non-terminal nodes (with two outgoing arcs (0 and 1) representing the occurrence/non-occurrence of variables), and arcs for the BDD model are defined respectively. The phase BDD model is constructed by manipulation rules, as:

$$g\diamondsuit h = ite(x,G_1,G_2)\diamondsuit casey(y,H_1,H_2) = \begin{cases} ite(x,G_1\diamondsuit H_1,G_1\diamondsuit H_1) & index(x)=index(y) \\ ite(x,G_1\diamondsuit h,G_2\diamondsuit h) & index(x)<index(y) \\ ite(y,g\diamondsuit H_1,g\diamondsuit H_2) & index(x)>index(y) \end{cases} \tag{10}$$

Step #2. Merge the phase BDD models into a system BDD model. The construction process of a two-phase example is shown in Figure 2. For variables representing the same components in different phases, the backward phase-dependent operation ($index(A_i)<index(A_j)$) is applied. The manipulation rule is shown as:

$$E_{Ai}\cdot E_{Aj} = ite(\overline{A}_i,G_1,G_2)\diamondsuit ite(\overline{A}_j,H_1,H_2) = ite(\overline{A}_j,E_{Ai}\diamondsuit H_1,G_2\diamondsuit H_2) \tag{11}$$

Step #3. With the system BDD model constructed in Step #2, derive all paths, η_{sys}, that lead to system success. For example, the success path for the example in Figure 2 is $\eta_{sys}=\overline{A}_2\overline{B}_1$ and accordingly the system reliability is modeled by $R_{sys}=\Pr(\eta_{sys})$.

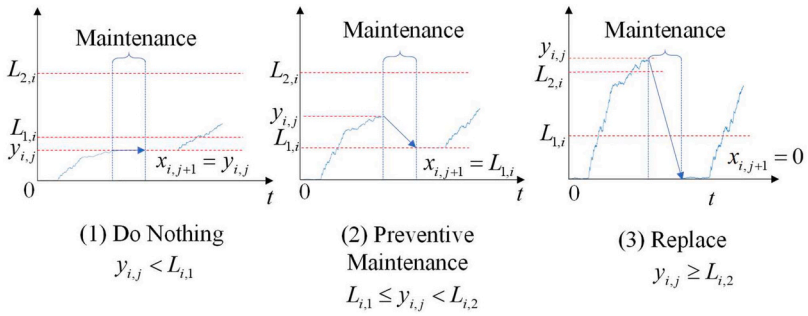

Figure 3. Maintenance actions and degradations of components.

2.3. Maintenance Modeling and Optimization

2.3.1. Maintenance modeling

For R-PMSs, maintenance actions are carried out during missions, that is, components will be checked and maintained so that the system can be ready for the $(k+1)$th mission after the completion of the kth$(k \ge 1)$ mission. An essential issue is to optimal allocation of maintenance resources to ensure that the system satisfies predefined performance and reliability. Specifically, $x_{i,j}$ and $y_{i,j}$ are degradation values of component i before and after the jth mission. Three maintenance actions are considered (see Figure 3):

(i) Do Nothing (DN). No maintenance actions will be implemented in case the degradation meets $y_{i,j} \le L_{1,i}$. The degradation for each component remains the same in the next mission (represented by $x_{i,j+1} = y_{i,j}$).
(ii) Preventive Maintenance (PM). The component will be maintained if the degradation meets $L_{1,i} \le y_{i,j} < L_{2,i}$, and the degradation will be updated to a lower-level as a result of the maintenance actions being implemented, say $x_{i,j+1} = L_{1,i}$.
(iii) Replace (RE). The component will be replaced with a new one with an updated degradation as $x_{i,j+1} = 0$ if the degradation follows $y_{i,j} \ge L_{2,i}$. Accordingly, for component i, the decision depends on $L_{1,i}$ and $L_{2,i}$, called the maintenance and replace criteria, respectively.

The degradation transition paths are derived as in Figure 4. Before the 1st mission, the degradation of component i is $x_{1,i} = 0$ and it degrades to possible sections, that are, $y_{1,i} \in (0, L_{1,i}), [L_{1,i}, L_{2,i}), [L_{2,i}, +\infty)$. With the maintenance strategies above, the degradation of component i reaches $x_{2,i} = y_{1,i}$, $x_{2,i} = L_{1,i}$ and $x_{2,i} = 0$, respectively.

It is noted that multiple paths are generated after several missions. For instance, Figure 4 shows 3^k paths for component i with k missions, resulting in a typical state explosion issue. To address this challenge, an approximation method based on degradation expectation is proposed to estimate the state probabilities of components following each mission. Two operational scenarios are subsequently introduced: unlimited/limited (number of) missions.

(a) Scenario #1: Unlimited Missions

In this scenario, all components in R-PMSs are replaceable or maintainable. The maintenance criteria $L_{1,i}$ remain the same in different missions. Accordingly, a system enters a stationary state after a few missions, and the components' state probabilities remain the same across the kth maintenance action, see Figure 5.

Figure 5 indicates that the probability of the degradation of component i in advance of kth mission ($\Pr_{x_{k,i}=0}$) is equal to 0. The expectation of the degradation of component i can be $\bar{L}_{k,i}$, 0, or $L_{1,i}$. The maintenance implemented resulting in the recovery of component i reaching 0 or $L_{1,i}$. It is pointed out that a larger degradation (say $>L_{1,i}$) generates $\bar{L}_{k,i} \in (0, L_{1,i})$. If the component is in a stationary state with the maintenance strategy $L_{1,i}, L_{2,i}$, the components' state probabilities and degradation expectation fulfill:

$$\begin{cases} \Pr_{x_{k,i}=0} = \Pr_{x_{k+1,i}=0}, & \Pr_{x_{k,i}=\bar{L}_{k,i}} = \Pr_{x_{k+1,i}=\bar{L}_{k+1,i}} \\ \Pr_{x_{k,i}=L_{1,i}} = \Pr_{x_{k+1,i}=L_{1,i}} & \bar{L}_{k,i} = \bar{L}_{k+1,i} \end{cases} \tag{12}$$

With the component's initial degradation $x_{k,i}$, the PDF of the $y_{k,i}$ is evaluated by Eq. (8), generating:

$$\begin{aligned} & f\left(y_{k,i} | (T_1, \cdots, T_M), x_{k,i}, (\mu_1, \cdots, \mu_M), (\sigma_1, \cdots, \sigma_M)\right) \\ = & \int_{-\infty}^{D} \int_{-\infty}^{D} \cdots \int_{-\infty}^{D} f_3\left(y_{k,i} | T_M, x_{k_{M-1},i}, \mu_M, \sigma_M\right) \cdots f_3\left(x_{k'',i} | T_2, x_{k_1,i}, \mu_2, \sigma_2\right) \\ & f_3\left(x_{k_1,i} | T_2, x_{k,i}, \mu_1, \sigma_1\right) dx_{k_1,i} dx_{k_2,i} \cdots dy_{k,i} \end{aligned} \tag{13}$$

In Eq. (13), $(T_1, \cdots, T_M)$, $(\mu_1, \cdots, \mu_M)$, and $(\sigma_1, \cdots, \sigma_M)$ are durations, drift, and diffusion coefficients of the component in different phases, $x_{k_j,i}$ denotes the component's degradation at the end of phase j of the kth mission. Accordingly, Eq. (13) is derived as:

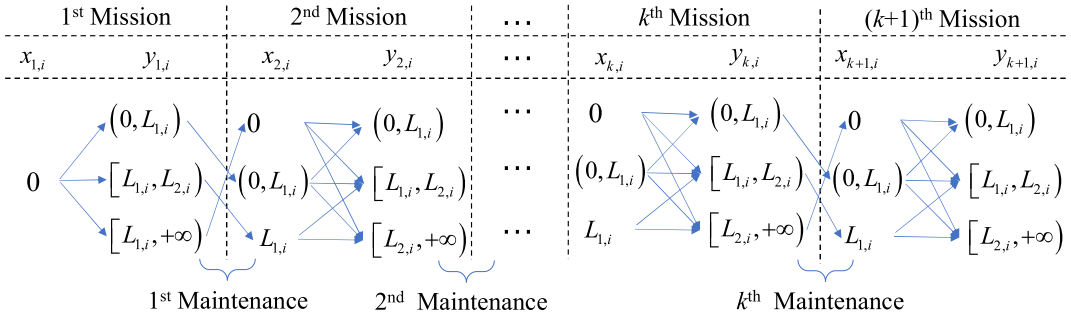

Figure 4. Possible paths for component i.

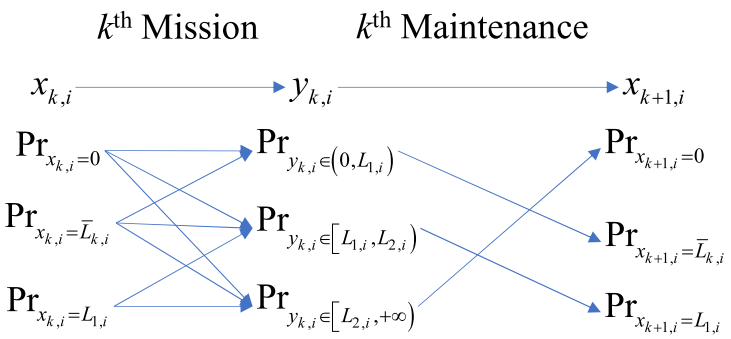

Figure 5. Stationary state probabilities of component i.

$$\begin{aligned}&\Pr_{x_{k+1,i}=0}\\&=\Pr\left(y_{y_{k,i}}\in[L_{2,i},+\infty)\right)\\&=\int_{L_{2,i}}^{+\infty}f\left(y_{k,i}|x_{k,i}=0\right)\Pr_{x_{k,i}=0}dy_{k,i}+\int_{L_{2,i}}^{+\infty}f\left(y_{k,i}|x_{k,i}=\bar{L}_{k,i}\right)\Pr_{x_{k,i}=\bar{L}_{k,i}}dy_{k,i}\\&\quad+\int_{L_{2,i}}^{+\infty}f\left(y_{k,i}|x_{k,i}=L_{1,i}\right)\Pr_{x_{k,i}=L_{k,i}}dy_{k,i}\end{aligned}\tag{14}$$

$$\begin{aligned}&\Pr_{x_{k+1,i}=\bar{L}_{k+1,i}}\\&=\Pr\left(y_{y_{k,i}}\in(0,L_{1,i})\right)\\&=\int_{0}^{L_{1,i}}f\left(y_{k,i}|x_{kT_M}=0\right)\Pr_{x_{k,i}=0}dy_{k,i}+\int_{\bar{L}_{k,i}}^{L_{1,i}}f\left(y_{k,i}|x_{kT_M}=\bar{L}_{k,i}\right)\Pr_{x_{k,i}=\bar{L}_{k,i}}dy_{k,i}\end{aligned}\tag{15}$$

$$\begin{aligned}&\Pr_{x_{k,i}=L_{1,i}}\\&=\Pr\left(y_{y_{k,i}}\in[L_{i,1},L_{i,2})\right)\\&=\int_{L_{1,i}}^{L_{2,i}}f\left(y_{k,i}|x_{k,i}=0\right)\Pr_{x_{k,i}=0}dy_{k,i}+\int_{L_{1,i}}^{L_{2,i}}f\left(y_{k,i}|x_{k}=\bar{L}_{k,i}\right)\Pr_{x_{k,i}=\bar{L}_{k,i}}dy_{k,i}\\&\quad+\int_{L_{1,i}}^{L_{2,i}}f\left(y_{k,i}|x_{k,i}=L_{1,i}\right)\Pr\left(x_{k,i}=L_{1,i}\right)dy_{k,i}\end{aligned}\tag{16}$$

$$\begin{aligned}\bar{L}_{k+1,i}&=\int_{0}^{L_{i,1}}y_{k,i}f\left(y_{k,i}|x_{k,i}=0\right)\Pr\left(x_{k,i}=0\right)dy_{k,i}\\&\quad+\int_{0}^{L_{i,1}}f\left(y_{k,i}|x_{kT_M}=\bar{L}_{k,i}\right)\Pr\left(x_{k,i}=\bar{L}_{k,i}\right)dy_{k,i}\end{aligned}\tag{17}$$

Eqs. (14)-(16) produce the probabilities of stationary component states, with which the stationary system maintenance cost $\bar{C}_{UF}(L)$ and time $\bar{T}_{UF}(L)$ for each maintenance are computed by:

$$\begin{aligned}\bar{C}_{UF}(L)&=\sum_{i=1}^{M}\left(C_{ins,i}+\bar{C}_{PM,i}+\bar{C}_{RE,i}\right)+\bar{C}_{Fail}\\\bar{C}_{PM,i}&=\int_{L_{i,1}}^{L_{i,2}}c_{PM,i}\left(y_{k,i}-L_{1,i}\right)f\left(y_{k,i}|x_{k,i}=0\right)\Pr_{x_{k,i}=0}dy_{k,i}\\&\quad+\int_{L_{i,1}}^{L_{i,2}}c_{PM,i}\left(y_{k,i}-L_{1,i}\right)f\left(y_{k,i}|x_{k,i}=\bar{L}_{k,i}\right)\Pr_{x_{k,i}=\bar{L}_{k,i}}dy_{k,i}\\&\quad+\int_{L_{i,1}}^{L_{i,2}}c_{PM,i}\left(y_{k,i}-L_{1,i}\right)f\left(y_{k,i}|x_{k,i}=L_{1,i}\right)\Pr_{x_{k,i}=L_{1,i}}dy_{k,i}\\\bar{C}_{RE,i}&=c_{RE,i}\Pr_{x_{k,i}=0},\qquad\bar{C}_{Fail}=\left(1-R_{sys}\right)c_{Fail}\end{aligned}\tag{18}$$

$$\begin{aligned}\bar{T}_{UF}(L)&=\sum_{i=1}^{M}\left(T_{ins,i}+\bar{T}_{IM,i}+\bar{T}_{RE,i}\right)+T_{Fail}\\\bar{T}_{PM,i}&=\int_{L_{i,1}}^{L_{i,2}}t_{PM,i}\left(y_{k,i}-L_{1,i}\right)f\left(y_{k,i}|x_{k,i}=0\right)\Pr_{x_{k,i}=0}dy_{k,i}\\&\quad+\int_{L_{i,1}}^{L_{i,2}}t_{PM,i}\left(y_{k,i}-L_{1,i}\right)f\left(y_{k,i}|x_{k,i}=\bar{L}_{k,i}\right)\Pr_{x_{k,i}=\bar{L}_{k,i}}dy_{k,i}\\&\quad+\int_{L_{i,1}}^{L_{i,2}}t_{PM,i}\left(y_{k,i}-L_{1,i}\right)f\left(y_{k,i}|x_{k,i}=L_{1,i}\right)\Pr_{x_{k,i}=L_{1,i}}dy_{k,i}\\\bar{T}_{RE,i}&=\Pr_{x_{k,i}=0}t_{RE,i},\qquad\bar{T}_{Fail}=\left(1-R_{sys}\right)t_{Fail}\end{aligned}\tag{19}$$

In Eqs. (18) and (19), $C_{ins,i}, \bar{C}_{PM,i}, \bar{C}_{RE,i}$ are costs of inspection, imperfect maintenance, and replacement of component i, $c_{PM,i}/c_{RE,i}$ and $t_{PM,i}/t_{RE,i}$ denote the preventive maintenance/replacement cost and time of component i, $\bar{C}_{Fail}$ and $\bar{T}_{Fail}$ are the failure penalty for the whole system, with which the optimization of the system reliability is formulated

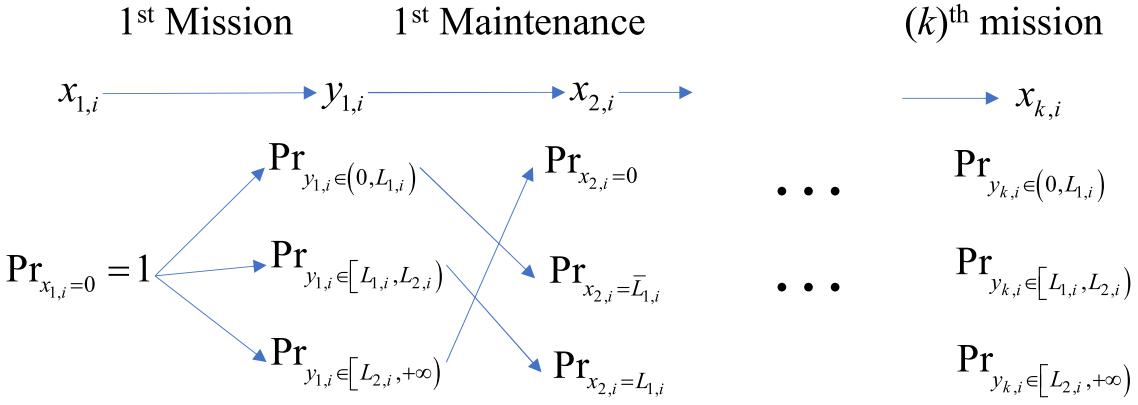

Figure 6. Stationary state probabilities of component i.

as:

$$\begin{aligned} &\max \quad R_{sys} = R_{sys}(L) \\ &s.t. \quad \begin{cases} \overline{T}_{UF}(L) \le T_{\max} \\ \overline{C}_{UF}(L) \le C_{\max} \end{cases} \end{aligned} \tag{20}$$

(b) Scenario 2: Limited Missions

In this scenario, specific components are eligible for maintenance or replacement, while others are non-repairable. For instance, for large-scale systems like offshore wind turbines, electronic components with small size are usually replaceable, but structural components with large sizes are not. The non-repairable components, however, can withstand a limited number of missions. Under this configuration, the transition of state probabilities is illustrated in Figure 6.

Figure 6 displays $K-1$ maintenance actions among K missions. The probabilities of the component's state are evaluated according to maintenance strategies $L_{1,i}$ (PM criteria) and $L_{2,i}$ (RE criteria). The cost $\overline{)C}_{LF}(L)$ and time $\overline{)T}_{LF}(L)$ for maintenance are evaluated by:

$$\begin{aligned} \overline{)C}_{LF}(L) &= \sum_{k=1}^{K}\left[\sum_{i=1}^{M}\left(C_{ins,i} + \overline{C}_{PM,k,i} + \overline{C}_{RE,k,i}\right) + \overline{C}_{Fail,k}\right] \\ \overline{)T}_{LF}(L) &= \sum_{k=1}^{K}\left[\sum_{i=1}^{M}\left(T_{ins,i} + \overline{T}_{PM,k,i} + \overline{T}_{RE,k,i}\right) + \overline{T}_{Fail,k}\right] \end{aligned} \tag{21}$$

Subsequently, the optimization is formulated as:

$$\begin{aligned} &\min \quad C = \overline{C}_{LF}(L) \\ &s.t. \quad \begin{cases} R_{sys}(L) \ge R_{\min} \\ \overline{T}_{LF}(L) \le T_{\max} \end{cases} \end{aligned} \tag{22}$$

2.3.2. Optimization Techniques

The maintenance model developed in Section 2.2 featured the optimization process as an NP-hard problem, where exhaustive enumeration of all possible solutions is computationally prohibitive. Heuristic algorithms have been applied to deal with these problems, such as Genetic Algorithm (GA) [33], Ant Colony Optimization (ACO) [35], Whale Optimization Algorithm (WOA) [42], and satin bower bird optimization (SBO)[43]. For instance, Li [42] improved upon the traditional WOA by integrating chaotic mapping and quantum theory, and demonstrated its superiority in solving the tidal-influenced berth and crane allocation model. Yang [43] proposes a chaotic quantum adaptive satin bowerbird optimizer (CQASBO) algorithm to solve the E-BUQC model, delivering efficient and reliable scheduling solutions for container port optimization. In this article, a joint optimization method combining GA and ACO is employed. To be specific, ACO simulates communication among ants through pheromones, allowing ant colonies to explore the solution space iteratively. The pheromone is deposited and updated along the paths. The solutions are evaluated by probabilistically selecting paths based on the local pheromone concentration and heuristic information. Equal probabilities are first assigned to each path for a single node. Then, the pheromones deposited on the chosen paths gradually evaporate over time. According to the foraging rules of the ant colony, subsequent ants

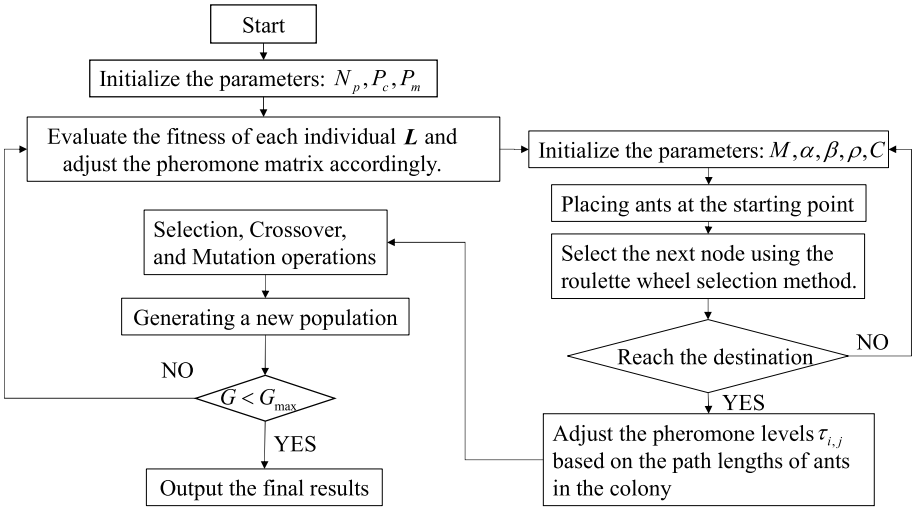

Figure 7. ACO-GA flowchart.

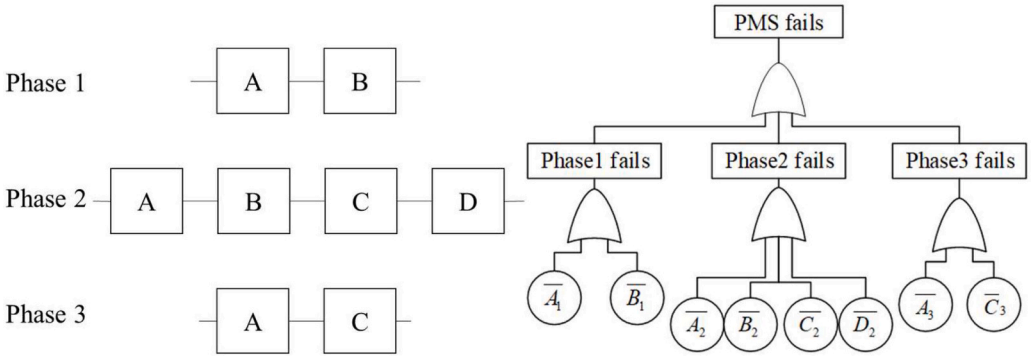

Figure 8. The RBD and FT models of Case #1.

Table 1
Reliability parameters for Case #1.

	A	B	C	D	Phase durations(days)
Phase 1	(0.4, 0.8)	(2, 1.5)	-	-	2
Phase 2	(0.8, 1)	(3, 1.5)	(0, 0.8)	(1, 1)	4
Phase 3	(0.6, 1.5)	-	(0.4, 1)	-	7
$D_{\max}$	10	16	9	6	-

Table 2
Maintenance parameters for Case #1.

	Cost			Time		
	$c_{ins,i}$	$c_{PM,i}$	$c_{RE,i}$	$t_{ins,i}$	$t_{PM,i}$	$t_{RE,i}$
A	0.05	0.25	5	0.02	0.25	0.2
B	0.02	0.12	2	0.05	0.54	0.5
C	0.04	0.22	4	0.03	0.32	0.3
D	0.03	0.19	3	0.02	0.25	0.2

will determine the next node based on the concentration of pheromones along the paths. The state transition probability of an ant between two nodes is expressed as:

$$p_{i,j}^{k}(t) = \begin{cases} \left[\tau_{i,j}(t)\right]^{\alpha}\cdot\left[\eta_{i,j}(t)\right]^{\beta} \Big/ \sum_{s\in allow}\left\{\left[\tau_{i,s}(t)\right]^{\alpha}\cdot\left[\eta_{i,s}(t)\right]^{\beta}, s\in S_{allow}\right. \\ 0, others \end{cases} \tag{23}$$

where, $\tau_{i,j}(t)$ denotes the pheromone concentration between nodes i and j at time t, while $\eta_{i,j}(t)$ represents the heuristic information for the path from node i to j at time t. The parameters α and β control the influence of pheromones and heuristics, S_{allow} signifies the range of feasible solutions.

It is necessary to identify the best solution to updating the pheromones after an iteration, which guides the search direction. The pheromones after the k-th iteration are expressed as:

$$\tau_{i,j}^{k} = \begin{cases} (1-\rho)\tau_{i,j}^{k-1} + C\Big/\zeta, & i,j\in\zeta \\ (1-\rho)\tau_{i,j}^{k-1} others \end{cases} \tag{24}$$

where, ρ represents the evaporation coefficient of the pheromone left behind, C is the scaling factor, p^{best} denotes the best solution, and ζ indicates the fitness of the optimal solution.

ACO is then integrated with GA to improve the solution efficiency, see Figure 7, where the structure of an individual is defined in Eq. (25). It is pointed out that the hybrid algorithm combines the positive feedback mechanism of ACO with the global search capabilities of GA, enabling it to quickly locate better solutions within a vast search space.

$$L = \begin{bmatrix} l_{a1}, l_{b1}, \cdots l_{n1} \\ l_{a2}, l_{b2}, \cdots l_{n2} \end{bmatrix} \tag{25}$$

3. Illustrations

This section provides both numerical and engineering analyses to validate the superiority of the proposed methodology. The numerical case demonstrates the correctness, efficiency, and sensitivity of the reliability and maintenance models, while the engineering case (a reusable launch vehicle attitude control system) examines the applicability and advantages of the proposed method over existing maintenance strategies.

3.1. Numerical Case (Case #1)

A numerical example is applied to illustrate the correctness and superiority of the proposed method. The system is composed of four components (A, B, C, D) and three phases for each mission. The system RBD and Fault Tree models are displayed in Figure 8. The reliability and maintenance parameters for the components are also shown in Tables 1 and 2. Accordingly, the system reliability modeling process by the proposed method is shown in Figure 9. In this case, all components are as good as new at the beginning of the first phase in the first mission. The components are subject to maintenance or replacement, and the system reaches a stationary state after several missions. The optimization algorithm, as shown in Eq.(20), is used to maximize system reliability within constraints of available budget and maintenance duration.

(a) Verification of System Reliability

An MC simulation procedure is applied as a basis to verify the proposed method, see Figure 10(a). It was run on a computer equipped with an Intel Core i5-10400 processor and 16GB of memory in the MATLAB (2021b) environment. The pseudo-code can be found in Appendix I. Compared to the MC method, the analytical approach proposed achieves a mean error of 0.0083, demonstrating its superior accuracy. Furthermore, the computation time required by the proposed method is 5.93s, outperforming that consumed by the MC method (104.56s), thereby highlighting its enhanced computational efficiency.

To address the inherent challenge of quantifying the exact degra-

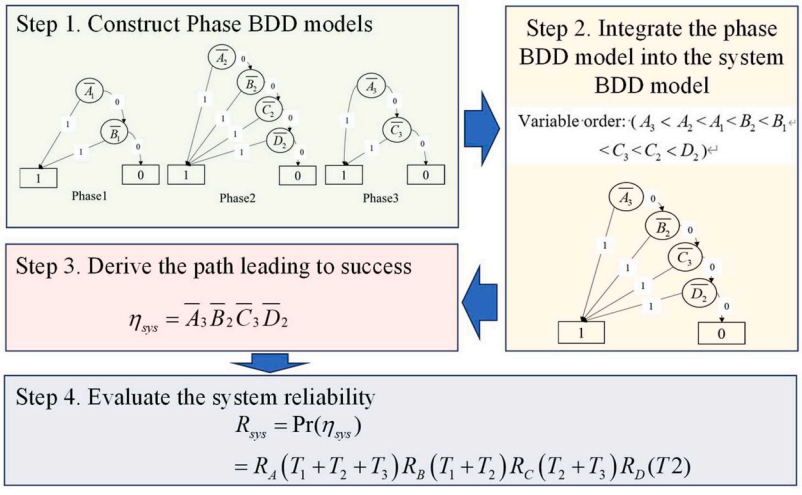

Figure 9. The reliability evaluation process.

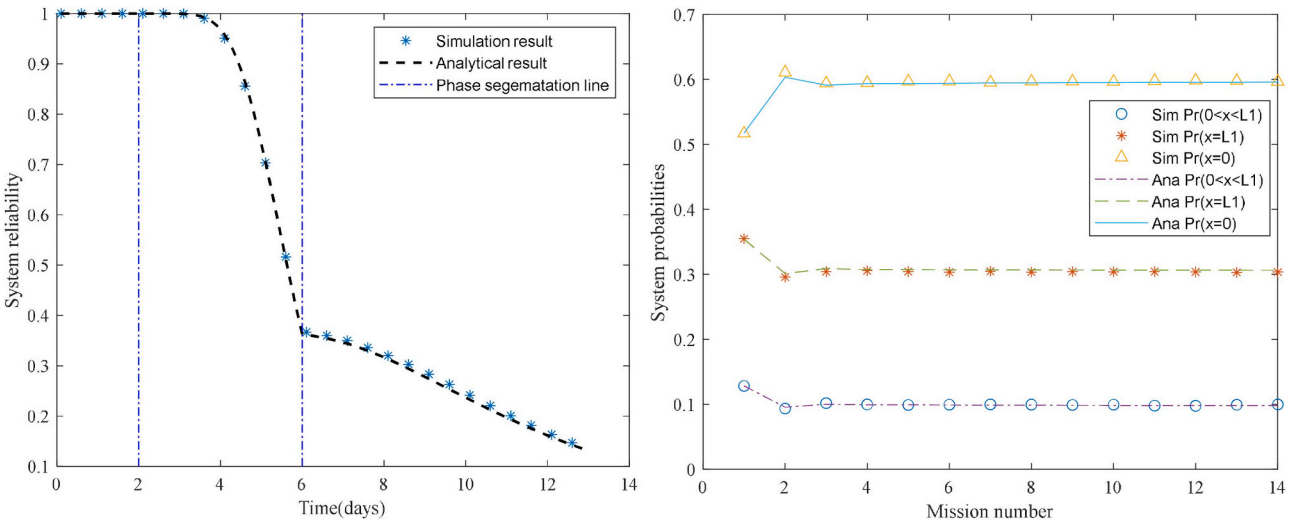

Figure 10. The results of system reliability analysis / (a) reliability of components under a simulation number of$N_{\max} = 2 \times 10^5$; (b) probabilities of states.

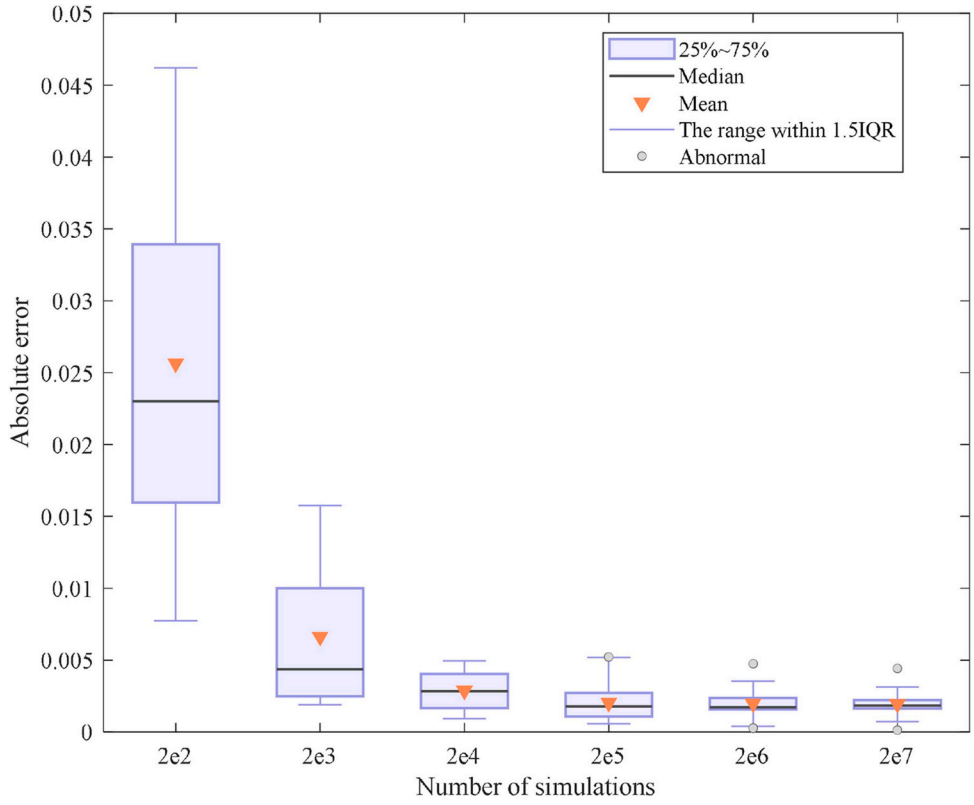

Figure 11. The error variation between the simulation and the analytical solutions.

dation levels in components governed by Wiener processes, Section 2.3.1 reformulates the problem into a probabilistic framework focusing on post-maintenance degradation states. MC simulation is employed to validate the accuracy of the methodology. Take component A as an example, with the maintenance strategies $L_{1,A} = 3$ and $L_{2,A} = 8$, the component state probabilities change with the order of missions, see Figure 10(b). Compared with the MC method, the average probability errors of the three states solved by the proposed method are 0.11×10^{-2}, 0.27×10^{-2}, and 0.21×10^{-2}, respectively. This indicates that the method can accurately describe the state changes of components after a maintenance has been taken.

Figure 11 illustrates the variation in error between the simulation-based and the proposed methods. The results demonstrate that the error consistently decreases with larger simulations. However, achieving higher accuracy through simulation requires a substantial increase in computational time and resources. In contrast, the proposed analytical method provides a deterministic solution that does not rely on repeated sampling, thereby eliminating the trade-off between precision and computational cost. The average error stabilizes at a low value of 0.0019, confirming that the analytical model maintains high accuracy

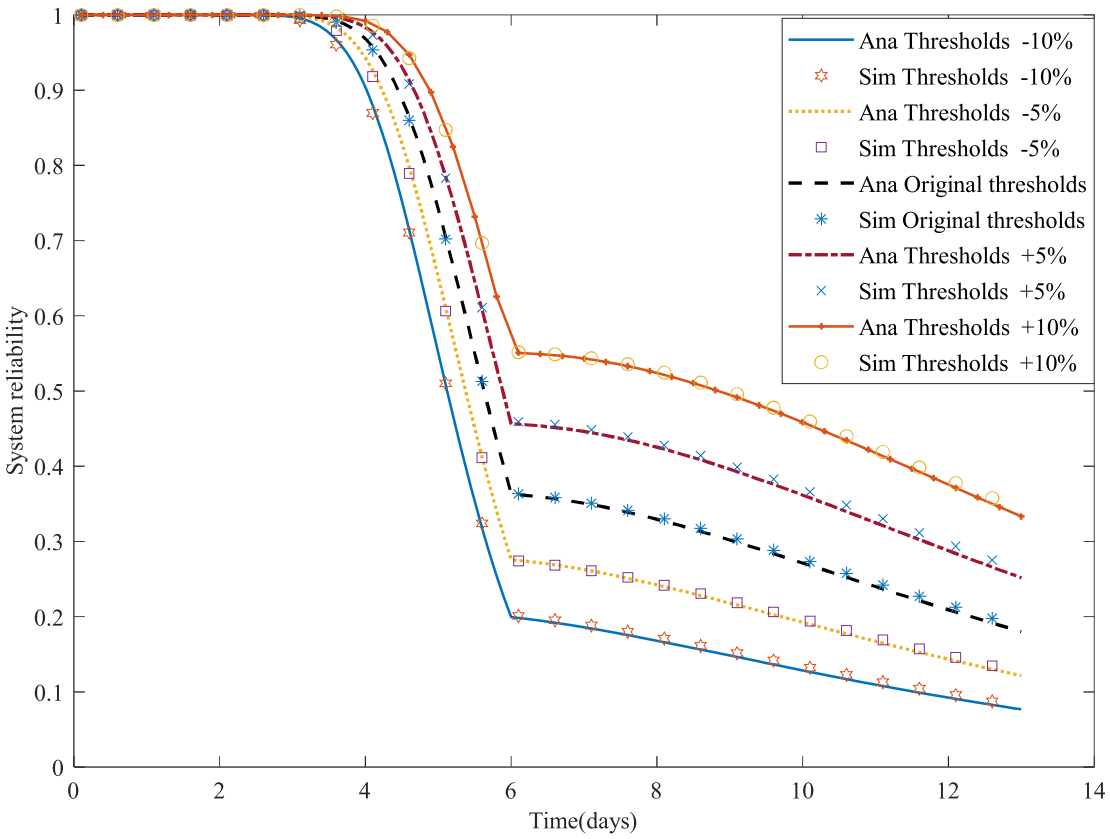

Figure 12. System reliability under a ±10% change in component thresholds.

Table 3
Optimal solutions for case #1 (Maintenance criteria setting for component).

	A	B	C	D
L_1	2.468	3.934	2.233	0.942
L_2	4.849	7.065	4.216	2.324

and reduces the computational burden compared to simulation-based approaches.

(b) Sensitive Analysis

A sensitivity analysis is also conducted to validate the accuracy and robustness of the proposed model under varying threshold conditions.

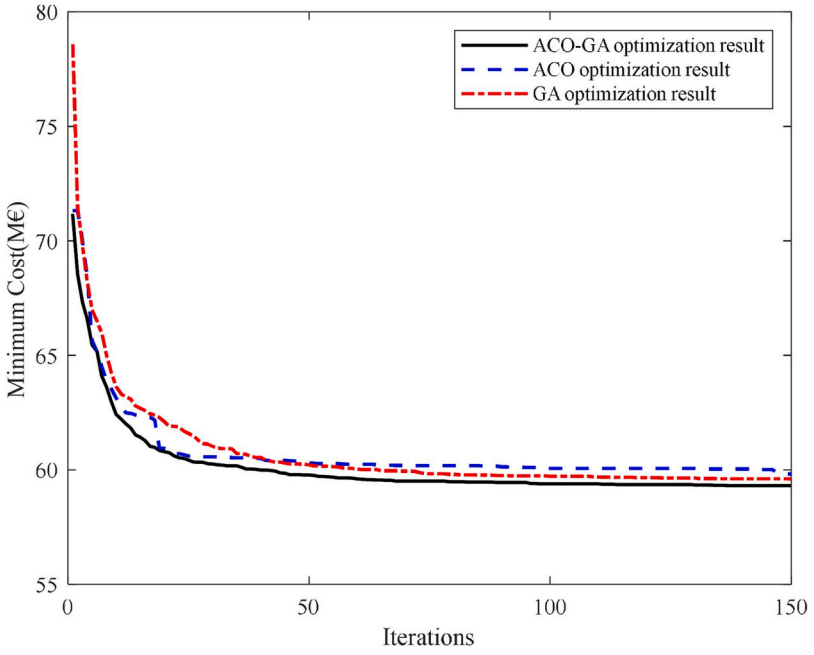

Figure 13. Comparison of three optimization algorithms.

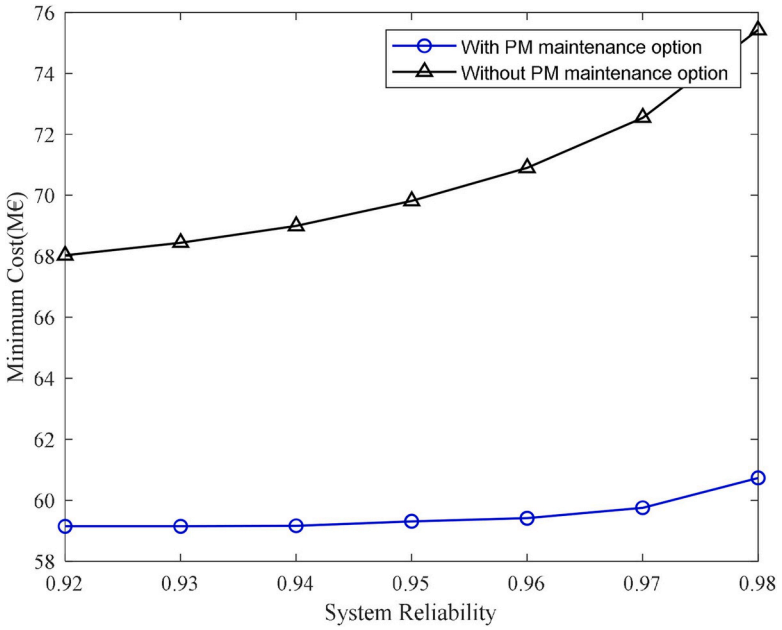

Figure 14. Comparison of maintenance strategies with and without PM.

As shown in Figure 12, the threshold parameters of all components in the system are varied by ±10%. The results indicate that system reliability exhibits the expected sensitivity to threshold variations. A decrease in thresholds leads to a certain degree of decline in the reliability curves. Moreover, across all tested scenarios, the analytical and simulated solutions remain highly consistent. This strongly demonstrates the correctness and stability of the proposed model, indicating that the findings are not coincidental and remain reliable even under reasonable parameter fluctuations.

(c) Verification of Maintenance Optimization

The parameters to drive the ACO-GA optimization include a crossover probability (0.7), the probability of variation (0.1), population size ($N = 20$), maximum iterations ($M_{\max} = 150$), genetic gap ($GGAP = 0.9$), number of ants ($m = 12$), pheromone factor ($\alpha = 2$), heuristic factor ($\beta = 1$), pheromone volatile factor ($\rho = 0.3$), the number of pheromone constants ($Q = 20$), system minimum reliability ($R_{\min} = 0.96$), and time constraints ($T_{\max} = 90$days). The optimized minimum maintenance cost is $C_{\min} = 59.38$M€, and the optimal maintenance strategy (maintenance criteria setting for each component) is shown in Table 3.

Furthermore, the ACO-GA is compared to the ACO and GA algorithms to verify its efficiency. The iterative results are carried out 10 times by these three methods, and their average results are shown in Figure 13. The ACO-GA hybrid algorithm demonstrates superior performance in both convergence behavior and solution quality. The ACO-GA method converges more rapidly in the early iterations, and it also achieves a significantly better final result, outperforming both the standalone ACO and GA approaches. This enhanced performance can be attributed to the effective integration of the positive feedback mechanism of ACO and the global exploitation strength of GA, which enables the hybrid method to escape local optima and consistently approach a near-optimal solution. The stable and efficient convergence trajectory further confirms the robustness and computational advantage of the ACO-GA framework in solving the target optimization problem.

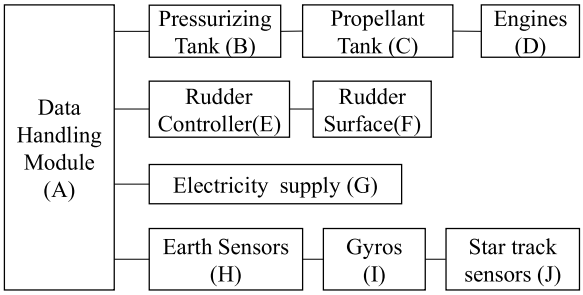

Figure 16. System configuration of the ACS.

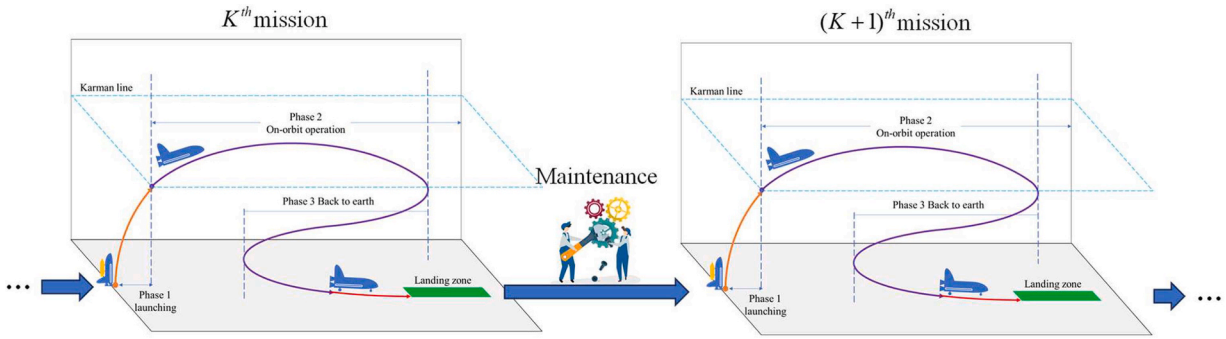

Figure 15. The multiple missions and maintenance procedures of RLVs.

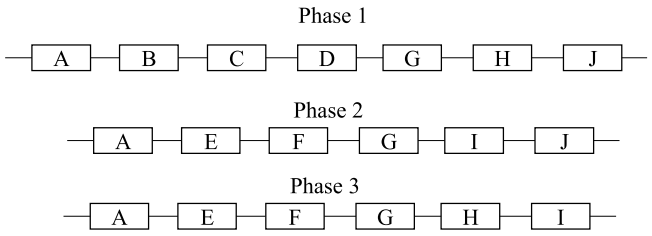

Figure 17. The RBD model for the ACS.

A comparative analysis is illustrated in Figure 14, by optimizing the maintenance costs with and without PM under system reliability constraints. The results indicate that PM reduces the overall maintenance cost, and a higher system reliability required generates a higher minimum maintenance cost.

3.2. Engineering Case (Case #2)

The astronautics Attitude Control System (ACS) in Reusable Launch Vehicle (RLV) is designed to control orbital parameters and attitude angles, ensuring the spacecraft maintains its designated trajectory and orientation throughout the mission lifecycle. For each mission, the ACS experience launching (phase #1), on-orbit operation (phase #2), and back to earth (phase #3) phases, see Figure 15. To be specific, in phase #1, the RLV is launched and separated; In phase #2, the RLV continues to work in outer space; In phase #3, the RLV returns to Earth. The recently emerged reusable RLV, completion of multiple series missions, requires the ACS to work in several missions till the end of design lifetime/decomposition, which featured the ACS as an R-PMS. The ACS consists of 10 components in four systems: Data Handling (A), Power Unit (B, C, D), Attitude Control (E, F), Electricity Supply (G), and sensors (H, I, J), see Figure 16.

The RBD models for these three phases are shown in Figure 17. The data in terms of the RLVs is in line with [20–22], see Table 4. The phase durations are $T_1 = 10h$, $T_2 = 240h$, $T_3 = 12h$.

Table 4. Accordingly, the system BDD model is constructed in Figure 18.

With the system BDD model, the system reliability is evaluated as:

$$\begin{aligned} R_{sys} &= \Pr(\eta_{sys}) \\ &= R_A(T_1+T_2+T_3)R_B(T_1)R_C(T_2)R_D(T_1) \\ &R_E(T_2+T_3)R_F(T_2+T_3)R_G(T_1+T_2+T_3) \\ &R_H(T_1+T_3)R_I(T_2+T_3)R_J(T_1+T_2) \end{aligned} \tag{26}$$

All components are as good as new at the commencement of the first phase. Between consecutive missions, maintenance actions are applied to corresponding components. In this scenario, components B, C, and D are limited to repair actions only, while the remaining components are eligible for both repair and replacement according to the nature of the system designed. The system is configured to operate over ten missions, after which the RLV will be decommissioned. Throughout the lifespan of the ACS, nine maintenance intervals are scheduled. To minimize the total system maintenance time, the corresponding optimization is

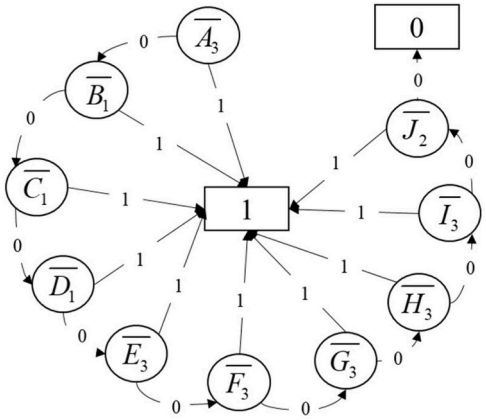

Figure 18. The BDD model for the ACS.

Table 5
Performance index for different components.

Component	PM/RE threshold	Index	Degradation assessment actions and performance index
A	$L_{1,A}$	4.236	Index: Degradation.
	$L_{2,A}$	4.849	Actions: Discrepancies between computational metrics and requirements.
B	$L_{1,B}$	2.614	Index: Degradation.
C	$L_{1,C}$	1.574	Actions: Surface crack clusters by non-destructive testing.
D	$L_{1,D}$	1.950	Index: Degradation. Actions: Degradation of the slowly varying components, isolated from raw signals by the slow feature analysis (SFA).
E	$L_{1,E}$	0.285	Index: Degradation.
	$L_{2,E}$	4.278	Actions: Output pulse voltage variations under diverse temperature stress levels.
F	$L_{1,F}$	1.467	Index: Degradation.
	$L_{2,F}$	3.779	Actions: Deflection angle alterations due to structural damage.
G	$L_{1,G}$	3.994	Index: Output voltage and discharge capacity.
	$L_{2,G}$	4.723	Actions: Constant-temperature discharge experiments.
H	$L_{1,H}$	1.587	Index: Sensor drift.
	$L_{2,H}$	2.298	Actions: Applying the principal component analysis (PCA), analyzing critical subsystems and synthesizing multidimensional data.
I	$L_{1,I}$	3.023	
	$L_{2,I}$	3.543	
J	$L_{1,J}$	3.992	
	$L_{2,J}$	5.769	

Table 4
Performance index for different components [20–22].

	Reliability parameters				Cost/(M€)		Time/(days)	
	(μ_1,σ_1)	(μ_2,σ_2)	(μ_3,σ_3)	$D_{\max}$	$c_{PM,i}$	$c_{RE,i}$	$t_{PM,i}$	$t_{RE,i}$
A	(0.4,0.8)	(0.8,1.0)	(0.6,1.5)	18	0.045	1.61	0.3	0.25
B	(0.5,0.8)	-	-	12	0.023	-	0.35	-
C	(0.4,1.0)	-	-	10	0.12	-	0.32	-
D	(0.6,0.9)	-	-	12	0.38	-	0.5	-
E	-	(1.0,0.7)	(1.2,1.0)	16	0.03	0.9	0.3	0.25
F	-	(0.6,0.8)	(1.0,1.2)	14	0.028	0.7	0.4	0.3
G	(0.5,0.8)	(0.5,1.0)	(1.2,1.5)	18	0.01	0.33	0.5	0.4
H	(0.6,0.7)	-	(1.0,1.0)	9	0.008	0.13	0.24	0.12
I	-	(0.4,0.4)	(1.2,1.0)	14	0.005	0.12	0.22	0.1
J	(0.5,0.8)	(0.8,1.2)	-	21	0.003	0.09	0.13	0.1

Table 6
Optimal solutions and comparison for the RLV with PM strategy.

Mission	$j=1$	$j=2$	$j=3$	$j=4$	$j=5$	$j=6$	$j=7$	$j=8$	$j=9$	$j=10$
$T^{s1}_{\min}$	6.21	6.38	6.49	6.64	6.85	7.06	7.25	7.43	7.62	-
C^{s1}_{j}	3.71	3.86	3.92	4.02	4.22	4.36	4.45	4.49	4.60	-
$R^{s1}_{sys,j}$	0.9791	0.9728	0.9682	0.9649	0.9624	0.9602	0.9583	0.9564	0.9549	0.9531

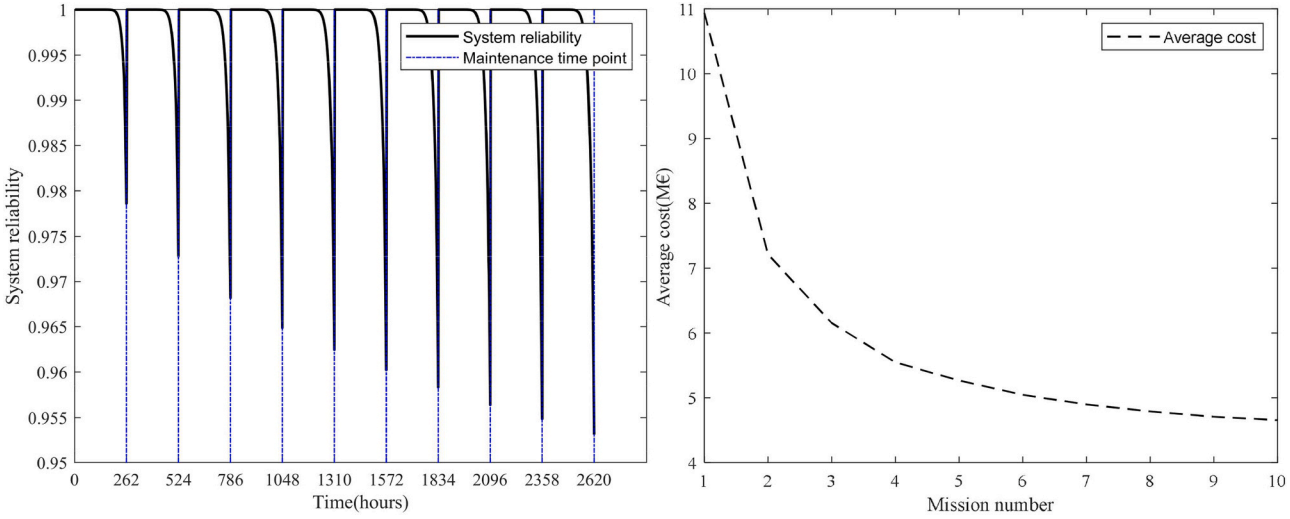

Figure 19. Analysis of missions of the RLV (a) System reliability; (b) Average cost.

Table 7
Optimal solutions for the RLV with strategies #2 and #3.

Mission		$j=1$	$j=2$	$j=3$	$j=4$	$j=5$	$j=6$	$j=7$	$j=8$	$j=9$	$j=10$
#2	$T^{s2}_{\min}$	7.92	9.00	9.33	9.45	9.56	9.67	9.76	9.92	10.11	-
	C^{s2}_{j}	3.69	3.96	4.15	3.95	3.97	4.01	4.07	4.20	4.37	-
	$R^{s2}_{sys,j}$	0.9791	0.9716	0.9683	0.9657	0.9637	0.9617	0.9599	0.9583	0.9569	0.9559
#3	$T^{s3}_{\min}$	8.09	8.08	7.63	7.34	7.05	6.87	6.70	6.59	6.49	-
	C^{s3}_{j}	3.82	4.08	4.15	4.12	4.19	4.19	4.20	4.30	4.44	-
	$R^{s3}_{sys,j}$	0.9791	0.9682	0.9610	0.9602	0.9595	0.9592	0.9588	0.9573	0.9516	0.9512

formulated as:

$$\begin{aligned} &\min \quad T = \overline{T}_{LF}(L) \\ &s.t. \quad \begin{cases} R_{sys,j}(L) \geq R_{\min} & 1 \leq j \leq 9 \\ \overline{C}_{LF}(L) \leq C_{\max} \end{cases} \end{aligned} \tag{27}$$

With the maximum budget $C_{\max} = 40\text{M}€$ and reliability constraint $R_{\min} = 0.95$, the minimal maintenance time reaches $T^{S1}_{\min} = 61.96$ *days*. Performance index for different components are displayed in Table 5 and the system maintenance time, cost and reliability after each mission are shown in Table 6.

The system reliability of the ACS in 10 missions/flights is demonstrated in Figure 19(a). As noted earlier, a primary advantage of the RLV lies in its ability to reduce the average cost across multiple missions. With the optimal solutions, the average cost for missions is computed in Figure 19(b), which shows that the average cost decreases sharply when the mission number is relatively low (from 1 to 5) but it becomes unobvious after the 6$^{\text{th}}$ mission.

It is noted that the optimal maintenance solution of the ACS allocates uneven maintenance expenditure for each maintenance activity. However, practical projects sometimes distribute even budget (the upper limit) for missions to release the burden in project management. To this end, strategy #2 (with evenly distributed budget) and strategy #3 (without PM) are computed and compared with the result of the proposed strategy, see Table 7. In strategy #2, the maintenance cost of each maintenance is 40M€/9=4.44 M€. The minimal maintenance time reaches $T^{S2}_{\min} = 84.75$*days*. The systematic compilation of maintenance time and cost parameters across mission iterations in Table 6 demonstrates critical operational insights for reusable aerospace systems. These quantitative parameters provide a flight-specific scheduling basis for inter-mission maintenance operations, enabling precise resource allocation at launch sites, logistics planning, and the implementation of quantifiable management frameworks. The progressive increase in maintenance duration (from 6.21 to 7.62 days) quantifies the operational complexity escalation induced by cumulative system degradation. Concurrently, the maintenance cost fluctuation (from 3.71 to 4.60 M€) reflects differentiated resource requirements across mission phases. This granular dataset facilitates the establishment of mission sequence-maintenance workload correlation models, forming a predictive foundation for mission cycle planning.

The comparative analysis in Table 7 substantiates the engineering efficacy of the proposed optimized strategy. Compared to Strategy #2, the dynamic resource distribution mechanism achieves a 20.8% reduction in average maintenance time, exposing the limitations of static fiscal controls in addressing actual degradation patterns. The contrast with Strategy #3 highlights preventive maintenance's critical role in reliability governance, while Strategy #3 exhibits minimal maintenance durations ($T^{s3}_{\min} = 64.85$days), its accelerated reliability decay directly compromises mission safety margins. The superiority of Strategy1, which optimizes maintenance thresholds based on a multi-phase degradation process, is thus confirmed to deliver a practical and

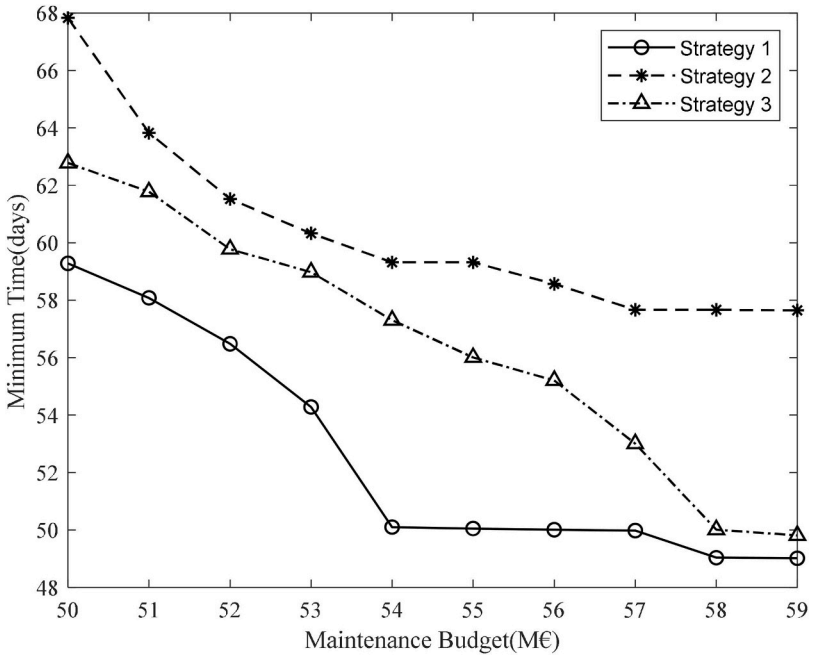

Figure 20. The optimal time for maintenance strategies under various budget constraints.

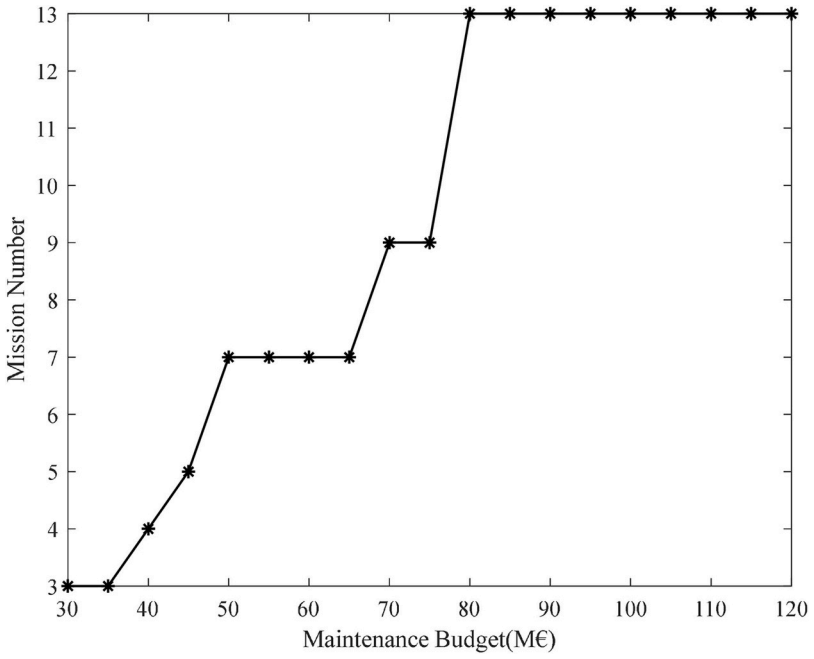

Figure 21. The maximum mission number with a different maintenance budget.

optimal trade-off between maintenance efficiency and system reliability for reusable aerospace systems.

Figure 20 indicates that maintenance time decreases with an increased budget, and drives the maintenance decisions toward RE. Strategy #2 exhibits the longest maintenance time across all budget ranges, reflecting how its imposed constraints limit the flexible allocation of maintenance resources, rendering it less efficient compared to the other strategies. Notably, strategy #1 outperforms strategy #3 across all budget ranges, achieving shorter maintenance time. As the maintenance budget increases, the gap in the minimum maintenance time between strategy #1 and strategy #3 gradually diminishes, primarily due to the system's reliance on RE to reduce downtime under elevated budgetary conditions. The comparison also concludes the following:

- An optimized constraint design ensures budget-driven maintenance plans align with minimal maintenance time targets across all strategies.
- An increase in maintenance budget shortens the maintenance cycle, but it becomes unclear if the budget investment exceeds a certain threshold.

Therefore, the budget allocation should be dynamically optimized. On the other hand, the determination of the best number of missions represents an open question for reusable systems. The maximum mission number with reliability ($R_{\min} = 0.96$) and budget (30M€ to 120M€) constraints is tested in Figure 21. It is concluded that an increased maintenance budget generates more efficient maintenance as well as

more allowable missions. As the maintenance budget increases incrementally from 30M€ to 120M€, the maximum reusable frequency of the RLV demonstrates an upward trend yet exhibits distinct phased characteristics in a growth rate. The budget-performance correlation is typical in complex system maintenance scenarios. Initial resource investments efficiently address systemic deficiencies, but as performance improves, technological ceilings gradually emerge.

Engineering efforts should prioritize data-driven modeling to delineate a high cost-effectiveness optimization zone-for instance, leveraging historical failure data to prioritize maintenance for high-risk components (e.g., engine health monitoring). Furthermore, maintenance strategies must align with design-phase optimizations, such as improving maintainability (modular architectures, rapid disassembly interfaces), to fundamentally reduce lifecycle costs.

4. Conclusions and future works

This paper proposes a reliability-centered maintenance optimization method for reliability modeling and maintenance planning of reusable phased mission systems (R-PMSs) with the assistance of a multi-phased Wiener process-based reliability modeling method and a Binary Decision Diagram-based model. This reflects the impacts of multiple usages of R-PMSs by defining the initial states of components to be perfect/imperfect fixed. The constructed maintenance model is able to optimally schedule maintenance actions between missions of R-PMSs. Two cases, a numerical case and an engineering case, illustrated the performance of the proposed method. The findings reveal that an increase in maintenance budget yields reductions in maintenance duration and enhancements in reusable mission frequency, while demonstrating diminishing marginal returns when the budget exceeds a critical threshold. Meanwhile, compared to evenly distributing the budget or not implementing preventive maintenance, the optimal maintenance strategy that allocates uneven maintenance expenditure across missions is more efficient in reducing maintenance time. The results confirm that the proposed method contributes to reliability modeling and maintenance scheduling of R-PMSs.

This study establishes a reliability assessment and maintenance framework for R-PMSs, focusing on their natural degradation. To extend the present work, future research will be directed along several promising avenues. Firstly, a valuable extension would be to incorporate the effects of external shocks, investigating their competing risks with the inherent degradation process. Secondly, integrating system availability into the evaluation framework would offer a more comprehensive metric aligned with practical engineering requirements. Thirdly, future research will explore the application of AI-based algorithms to enhance the adaptability and precision of maintenance decision-making, such as deep reinforcement learning, machine learning, etc.

CRediT authorship contribution statement

Xiang-Yu Li: Writing – original draft, Methodology, Investigation, Funding acquisition, Data curation. **Haochen Wang:** Validation, Methodology, Investigation, Formal analysis. **He Li:** Writing – original draft, Formal analysis, Conceptualization. **Xiaoyan Xiong:** Visualization, Resources, Investigation. **Zaili Yang:** Writing – review & editing, Formal analysis. **Hong-Zhong Huang:** Writing – original draft, Conceptualization. **Michael Beer:** Writing – original draft, Methodology. **Jin Wang:** Writing – original draft, Supervision.

Declaration of competing interest

This is no Conflict of Interests.

Acknowledgments

This study is sponsored by the National Natural Science Foundation of China under Grant No. 72101173 and the Natural Science Foundation of ShanXi Province under Grant No. 20210302124442.

Appendix I

Monte Carlo simulation for the three-stage degradation process

Input:
Number of simulations M,
Time interval dt,
Failure threshold$D$,
Initial degradation x_0, durations for three phases T_1, T_2 and T_3,
Degraded parameters for three phases (μ_1,σ_1), (μ_2,σ_2) and (μ_3,σ_3).

Body:
$numberofsurvivals = zeros(1,(T_1 + T_2 + T_3)/dt + 1)$
for $k = 1$to$M$:
$X(1) = x_0$
$step = 0$
while $X(end) \le D$:
$currenttime = step * dt$
if $currenttime \le T_1$ then $dX = normrnd\left(u_1 * dt, \sigma_1 * \sqrt{dt}\right)$
elseif $T_1 < currenttime \le T_2$ then $dX = normrnd\left(u_2 * dt, \sigma_2 * \sqrt{dt}\right)$
else $dX = normrnd\left(u_3 * dt, \sigma_3 * \sqrt{dt}\right)$
end if
$X(end+1) = X(end) + dX$
$step = step + 1$
$numberofsurvivals(step) = numberofsurvivals(step) + 1$
if $currenttime = T_1 + T_2 + T_3$ then break while
end while
end for
$R(t) = numberofsurvivals./M$
return $R(t)$

Output:
Reliability function at time points t ($R(t)$).

Data availability

Data will be made available on request.

References

[1] Zang X, Sun N, Trivedi K S. A BDD-based algorithm for reliability analysis of phased-mission systems. IEEE Transactions on Reliability 1999;48(1):50–60.
[2] Huang H Z, Li H, Shi Y, et al. Theory and application of possibility and evidence in reliability analysis and design optimization. Journal of Reliability Science and Engineering 2025;1(1):015007.
[3] La Band R A, Andrews J D. Phased mission modelling using fault tree analysis. Proceedings of the Institution of Mechanical Engineers, Part E: Journal of Process Mechanical Engineering 2004;218(2):83–91.
[4] Shrestha A, Xing L, Dai Y. Reliability analysis of multistate phased-mission systems with unordered and ordered states. IEEE Transactions on Systems, Man, and Cybernetics-Part A: Systems and Humans 2010;41(4):625–36.
[5] Li X Y, Li X, Feng J, et al. Reliability analysis and optimization of multi-phased spaceflight with backup missions and mixed redundancy strategy. Reliability Engineering & System Safety 2023;237:109373.
[6] Li X Y, Huang H Z, Li Y F. Reliability analysis of phased mission system with non-exponential and partially repairable components. Reliability Engineering & System Safety 2018;175:119–27.
[7] Mu H N, Liu J W, Lu M C, et al. Reliability analysis method of phased-mission nuclear power equipment based on goal oriented methodology. //. In: 2016 IEEE International Conference on Industrial Engineering and Engineering Management (IEEM). IEEE; 2016. p. 1375–9.
[8] Pedar A, Sarma V V S. Phased-mission analysis for evaluating the effectiveness of aerospace computing-systems. IEEE Transactions on Reliability 2009;30(5):429–37.
[9] Burdick G R, Fussell J B, Rasmuson D M, et al. Phased mission analysis: A review of new developments and an application. IEEE Transactions on Reliability 2009;26(1):43–9.
[10] Ma Z, Wang G. Powered–coasting–powered multi-phase mission reconfiguration method for launch vehicles under power system failures. Advances in Space Research 2025;75(1):704–17.
[11] World Health Organization. Medical equipment maintenance programme overview//Medical equipment maintenance programme overview. 2011.
[12] Pillai J R, Rao M M, Bhanumathy P, et al. Mission design and performance of RLV-TD. Current Science 2018:101–8.
[13] Siesjoe J. An Underwater Robotics Platform for Hybrid AUV/ROV Systems. //. In: Offshore Technology Conference. OTC; 2018. D041S054R005.
[14] Jia X, Cao W, Hu Q. Selective maintenance optimization for random phased-mission systems subject to random common cause failures. Proceedings of the Institution of Mechanical Engineers, Part O: Journal of Risk and Reliability 2019;233(3):379–400.
[15] Goyal V, Wongchote J, Strizzi J D. Advancements in mission assurance standards for expendable and reusable launch vehicles. Journal of Aerospace Information Systems 2022;19(11):699–704.
[16] Watcharasitthiwat K, Wardkein P. Reliability optimization of topology communication network design using an improved ant colony optimization. Computers & Electrical Engineering 2009;35(5):730–47.
[17] Chen T, Li J, Jin P, et al. Reusable rocket engine preventive maintenance scheduling using genetic algorithm. Reliability Engineering & System Safety 2013;114:52–60.
[18] Jin P, Chen Z, Li R, et al. Opportunistic preventive maintenance scheduling for multi-unit reusable rocket engine system based on the variable maintenance task window method. Aerospace Science and Technology 2022;121:107346.
[19] Soares G. Reliability and Cost Modeling of Reusable Launch Vehicles. TU Delft; 2022. https://resolver.tudelft.nl/uuid:35d791b1-d613-4c2e-9faf-a0f67b435d2d.
[20] Liu Y, Huang H Z, Jiang T. Selective Maintenance for Multi-state Systems Under Imperfect Maintenance. //. Selective Maintenance Modelling and Optimization: Basic Methods and Some Recent Advances. Cham: Springer International Publishing; 2023. p. 45–63.
[21] Levitin G, Lisnianski A. Joint redundancy and maintenance optimization for multistate series–parallel systems. Reliability Engineering & System Safety 1999;64(1):33–42.
[22] Liao R, He Y, Feng T, et al. Mission reliability-driven risk-based predictive maintenance approach of multistate manufacturing system. Reliability Engineering & System Safety 2023;236:109273.
[23] Zeng Y, Huang T, Zhang T, et al. System-level performance degradation prediction for power converters based on SSA–Elman NN and empirical knowledge. IEEE Transactions on Industrial Informatics 2023;20(2):1240–50.
[24] Dao C D, Zuo M J. Selective maintenance of multi-state systems with structural dependence. Reliability engineering & system safety 2017;159:184–95.
[25] Zhang L, Chen X, Khatab A, et al. Optimizing imperfect preventive maintenance in multi-component repairable systems under s-dependent competing risks. Reliability Engineering & System Safety 2022;219:108177.
[26] Feng X, Chen X, Zhao S. Optimizing multilevel maintenance in multi-component systems under s-dependent competing risks. IFAC-PapersOnLine 2024;58(19):1246–51.
[27] Liu L, Yang J, Kong X, et al. Multi-mission selective maintenance and repair persons assignment problem with stochastic durations. Reliability Engineering & System Safety 2022;219:108209.
[28] Khatab A, Aghezzaf E H, Djelloul I, et al. Selective maintenance optimization for systems operating missions and scheduled breaks with stochastic durations. Journal of Manufacturing Systems 2017;43:168–77.
[29] Lust T, Roux O, Riane F. Exact and heuristic methods for the selective maintenance problem. European journal of operational research 2009;197(3):1166–77.
[30] Xu Q, Wang Z, Jiang C, et al. Data-driven predictive maintenance framework considering the multi-source information fusion and uncertainty in remaining useful life prediction. Knowledge-Based Systems 2024;303:112408.
[31] Ruiz-Rodríguez M L, Kubler S, Robert J, et al. Dynamic maintenance scheduling approach under uncertainty: Comparison between reinforcement learning, genetic algorithm simheuristic, dispatching rules. Expert Systems with Applications 2024;248:123404.
[32] Chew S P, Dunnett S J, Andrews J D. Phased mission modelling of systems with maintenance-free operating periods using simulated Petri nets. Reliability Engineering & System Safety 2008;93(7):980–94.
[33] Distefano S, Puliafito A. Reliability and availability analysis of dependent-dynamic systems with DRBDs. Reliability Engineering & System Safety 2009;94(9):1381–93.
[34] Xing L, Meshkat L, Donohue S K. Reliability analysis of hierarchical computer-based systems subject to common-cause failures. Reliability Engineering & System Safety 2007;92(3):351–9.
[35] Li X Y, Huang H Z, Li Y F, et al. A Markov regenerative process model for phased mission systems under internal degradation and external shocks. Reliability Engineering & System Safety 2021;215:107796.
[36] Li X Y, Li X, Feng J, et al. Reliability analysis and optimization of multi-phased spaceflight with backup missions and mixed redundancy strategy. Reliability Engineering & System Safety 2023;237:109373.
[37] Lu J M, Wu X Y, Liu Y, et al. Reliability analysis of large phased-mission systems with repairable components based on success-state sampling. Reliability Engineering & System Safety 2015;142:123–33.
[38] Yu H, Wu X, Wu X. A combinatorial modeling method for mission reliability of phased-mission system with phase backups. IEEE Transactions on Reliability 2020;70(2):590–601.
[39] Cheng C, Yang J, Li L. Reliability assessment of multi-state phased mission systems with common bus performance sharing considering transmission loss and performance storage. Reliability Engineering & System Safety 2020;199:106917.
[40] Cheng C, Yang J, Li L. Reliability evaluation of a k-out-of-n (G)-subsystem based multi-state phased mission system with common bus performance sharing subjected to common cause failures. Reliability Engineering & System Safety 2021;216:108003.
[41] Qian C, Li Y, Zhu Y, et al. Remaining useful life prediction considering correlated multi-parameter nonlinear degradation and small sample conditions. Computers & Industrial Engineering 2025:111567.
[42] Li M W, Xu R Z, Yang Z Y, et al. Optimizing berth-crane allocation considering tidal effects using chaotic quantum whale optimization algorithm. Applied Soft Computing 2024;162:111811.
[43] Yang Z Y, Cao X, Xu R Z, et al. Applications of chaotic quantum adaptive satin bower bird optimizer algorithm in berth-tugboat-quay crane allocation optimization. Expert Systems with Applications 2024;237:121471.